Cement and Concrete Composites 74 (2016) 100–108

Contents lists available at ScienceDirect

Cement and Concrete Composites

journal homepage: www.elsevier.com/locate/cemconcomp

Development of solid state embeddable reference electrode for corrosion monitoring of steel in reinforced concrete structures

V. Maruthapandian [a, b, *], V. Saraswathy [a, b], S. Muralidharan [a]

[a] Corrosion and Materials Protection Division, CSIR - Central Electrochemical Research Institute, Karaikudi 630 003, Tamil Nadu, India
[b] Academy of Scientific and Innovative Research (AcSIR), New Delhi 110 025, India

ARTICLE INFO

Article history:
Received 23 February 2016
Received in revised form
28 August 2016
Accepted 3 September 2016
Available online 5 September 2016

Keywords:
Concrete
Steel reinforced concrete
Polarization
Alkaline corrosion
Potential parameter
Pourbaix diagram

ABSTRACT

Corrosion of steel reinforcement concrete structures is monitored through the surface mounting techniques using liquid based reference electrodes. Due to the limited usage of liquid based reference electrodes solid state reference electrode are introduced recently. In the present study, we fabricated and characterized Mn_3O_4 based pellet electrode for corrosion assessment of steel rebar in high alkaline medium through electrochemical methods and the results are compared with conventional saturated calomel reference electrode (SCE). The results indicate that the fabricated pellet electrode exhibits better characteristics suitable for high alkaline concrete environment and differentiate the passive and active status of steel rebar.

© 2016 Elsevier Ltd. All rights reserved.

1. Introduction

Steel reinforced concrete structures are plays a vital role in civil infrastructures such as bridges, dams and buildings. Steel reinforcement gives structural strength, stability, durability etc. Usually the pH of concrete structures is found highly alkaline (~12.5–13.5). This high alkaline pH produces a passive film on the surface of steel and hinders the further corrosion [1]. Though, the effect of external pollutants in concretes such as chloride ions, sulphate ions and CO_2 ingression affect the pH and induced the localized corrosion on the surface of steel rebar and promote the corrosion [2,3].

Prior detection and monitoring corrosion of steel in reinforced concrete structures pave the way to evaluate the lifespan of civil structures and take appropriate rehabilitation aspect. The non-destructive electrochemical corrosion monitoring methods such as galvanic potential measurement [4,5] open circuit potential measurements, linear polarization measurements and electrochemical impedance provides effective information on corrosion status [6,7] of rebar in concrete. In these methods, the rebar potential was measured with respect of standard reference electrodes like Ag/AgCl, Hg/Hg_2Cl_2 and $Cu/CuSO_4$ [8]. This reference electrode is consist of liquid part of either saturated chloride or sulphate solutions and made up of glass body as one part of it. These types of glass based liquid filled reference electrodes are not suitable for in-situ measurements [2] because the liquid part chloride and sulphate ions of solution leakage contaminate the concrete structure and induce the localized corrosion. In another way, most of the measurements were carried out by surface mounting techniques as per ASTM C876. This surface mounting technique may produce the erratic signal, non-reliable potential etc. due to the large distance of steel in concrete structures and outer surface.

To overcome these issue, embeddable pseudo reference electrodes and solid state reference electrodes is introduced by several groups [9–16]. Pseudo reference electrode (Quasi reference electrode) is a kind of reference electrode, in which their potentials were not stable, were dependent on various factors and the potential was not usually defined (Thermodynamic equilibrium cannot exist) approximately constant under appropriate conditions. Pt and Mo wire, Ag wired covered by Ag-salt of chloride and bromide is used in this typically as pseudo reference electrode in various fields which includes of corrosion monitoring of concrete structure [14]. In solid state reference electrode, the major components of sensing materials and embodiments are solid and it is used to measure the potential of other components (i.e. to be used

* Corresponding author. Corrosion and Materials Protection Division, CSIR - Central Electrochemical Research Institute, Karaikudi 630 003, Tamil Nadu, India.
E-mail address: maruthuori.tn@gmail.com (V. Maruthapandian).

http://dx.doi.org/10.1016/j.cemconcomp.2016.09.001
0958-9465/© 2016 Elsevier Ltd. All rights reserved.

potential measurements instead of conventional reference electrodes) [17–21]. These embeddable reference electrode have numerous advantages than compared to the liquid based reference electrodes [2,22–25] and that are usable for in-situ measurements due to their, smaller size, quick response, long self-life, maintenance free use and applicable to non-aqueous medium applications.

In concrete structures, the embeddable reference electrodes for corrosion monitoring of steel attracted by many researchers due to its reliable status of rebar due to minimized large distance between outer cover and inner steel rebar surface (minimize i_R drops) and it can be usable for long term monitoring on the basis of maintenance free use and also suitable for online monitoring due to their maintenance free nature [13–15].

In this embeddable reference electrodes most of the system used metal-metal oxide one of the components and which serves as main functions to produce stable potential in particular medium. In the case of MnO_2 and $NiFe_2O_4$ embeddable reference electrode [9–12], MnO_2 and $NiFe_2O_4$ were used as main components in PVC tube substrate sealed with porous cement plug; high alkaline paste (mixture of KOH, NaOH and $Ca(OH)_2$) act as conducting medium. Here the active materials are also deviated from the real concrete medium and the high solubility of alkaline and alkaline earth metal creates lake of connectivity between the concrete and sensing materials. In another case, G. S. Duffo et al. developed embeddable multi probe sensor based on mixed metal oxide probe as one of main components [13,14]. In which, there, rare earth high cost Ir, Ta and graphite rod from dry cell are used. The high cost and low inadequate availability of Ir and Ta not favored to commercialization. The graphite rod producing potential is questionable in high alkaline medium. In these aspects, the development of another active corrosion monitoring reference electrode is important and interesting. This is offers new kind of reference electrodes in this field.

Mn_3O_4 is a unique mixed metal oxide spinels due to coexistence of Mn in different valence state of Mn^{2+}, Mn^{3+} and used in many technological applications such as gas sensor, molecular adsorption, catalyst [25], lithium ion batteries [26] and used in various other aqueous, non-aqueous and high alkaline medium [27] due to their excellent physicochemical stability, non-toxic nature, low cost and high abundance.

Major objective of this work is to develop and characterize a solid state metal oxide reference electrode for corrosion assessment of steel in reinforced concrete structure. Hence, we described the fabrication of Mn_3O_4 based solid state metal oxide pellet reference electrode preparation and its electrochemical characterization in high alkaline environment and the effective use of corrosion monitoring of steel in reinforced concrete structures. Based on this study, the Mn_3O_4 pellet electrode provides unique and reliable potential applications with respect to SCE.

2. Materials and methods

2.1. Mn_3O_4 preparation

All the reagents used in this work were analytical grades and were used without further purifications. Double distilled water was used in all the experiments. Mn_3O_4 was synthesized through the metal chloride precipitation method and typically described as follows.0.22 mol of $MnCl_2 \cdot 2H_2O$ and 0.44 mol NaOH were separately dissolved in distilled water. Then NaOH solution was added to the $MnCl_2$ solution with constant stirring. After that, 1.37 m mol of cetyltrimethylammonium bromide (CTAB; cationic surfactant it enhances the formation of nanoparticles and suppress the reunion of nanoparticles [28]) was dispersed into the mixtures. The resulting precipitate was collected and washed with distilled water until the washing water amperes as neutral pH and then washed with ethanol. Finally the prepared sample was dried at 60° C for 24 h.

2.2. Characterizations

Structural characterization was performed by X-ray diffractometry using PAN elliptical D8 advance Diffractometer Cu Kα radiation with wavelength of 1.5406 Å. Fourier transform infrared spectra (FTIR) was recorded by Bruker-tensor 27 with opus 6.5 version software. The surface morphology of prepared sample was observed by scanning electron microscopy (SEM) through VEGA3 SB TESCAN SEM and Field-emission scanning electron microscopy (FE-SEM) using a Carl Zeiss AG Supra 55VP with an acceleration voltage of 5–30 kV. Phase composition were studied by Energy dispersive X-ray spectroscopic (EDS) method; which was collected using X-Flash Detector 410M with Bruker ESPRIT QUANTAX EDS analyzing software.

2.3. Fabrication of solid reference electrode

Solid state reference electrodes were prepared in PVC epoxy mold as follows. As prepared 0.5 g of Mn_3O_4 powder was mixed with 1% PVA in water (Polyvinyl alcohol) in agate mortar until got homogeneous dryness and then pressed into a pellet of 10 mm dia with thickness ~3 mm through hydraulic pressing machine (10 MPa). The electrical connection was made using Teflon coated copper wire with silver paste glue and embedded into PVC (polyvinylchloride) body using epoxy resin and it can be shown in Fig. 5a. Before evaluating the performance of Fabricated Pellet Electrode (FPE), which was polished by fine grade emery, papers in order to get the homogeneous exposure in test solutions.

2.4. Potential stability measurements for FPE

Potential stability of FPE in different pH solution (phosphate buffer), synthetic concrete pore solution (SCPS) (0.3 M KOH, 0.1 M NaOH and 0.01 M $Ca(OH)_2$; pH ~13) and 0.1 M NaOH were measured with respect to SCE in two electrode setup with help of high impedance multimeter. The FPE were immersed in test solution throughout the measured periods in a beaker and then salt bridge were used between the connection of working electrode (FPE) and the reference electrode of SCE. In each reading were taken out after attain the stability of ±5 mV.

2.5. Steel corrosion monitoring in solution medium

In order to evaluate the practical utility of fabricated electrode in concrete environment, we took steel rebar (5 cm length and 8 mm dia) in high alkaline pH medium of 0.1 M NaOH for passive medium and 0.1 M NaOH with 1% and 2% of NaCl for active medium.

2.6. Electrochemical studies for corrosion monitoring of steel rebar in solution medium

Potential of steel rebar (working electrode) was periodically measured with respect to the SCE (Saturated Calomel Electrode) and FPE through the two electrode cell setup. All the potential studies were measured in room temperature (30 ± 2 °C).

Potentiodynamic polarization and impedance studies were done using Gill automated potentiostat (ACM instrument, UK) in three electrode cell setup in which steel rebar served as working electrode, Pt foil (1 cm^2) served as counter electrode and SCE served as reference electrode. Similar experiments were also performed using FPE instead of SCE for the comparison purpose. In each measurement, the open circuit potential (OCP) was measured for

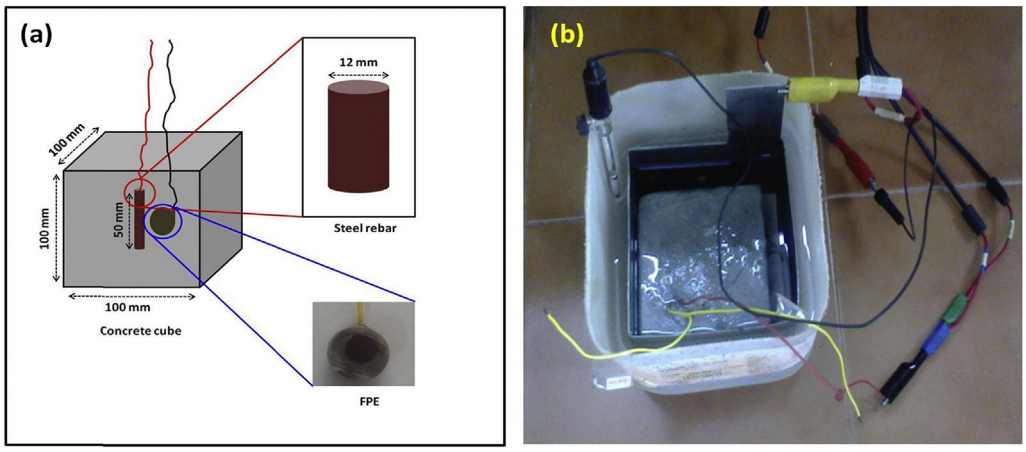

Fig. 1. (a) Schematic illustration of casted concrete cube with embedded FPE and (b) electrochemical studies setup of concrete cube embedded and ex-situ reference electrode of SCE.

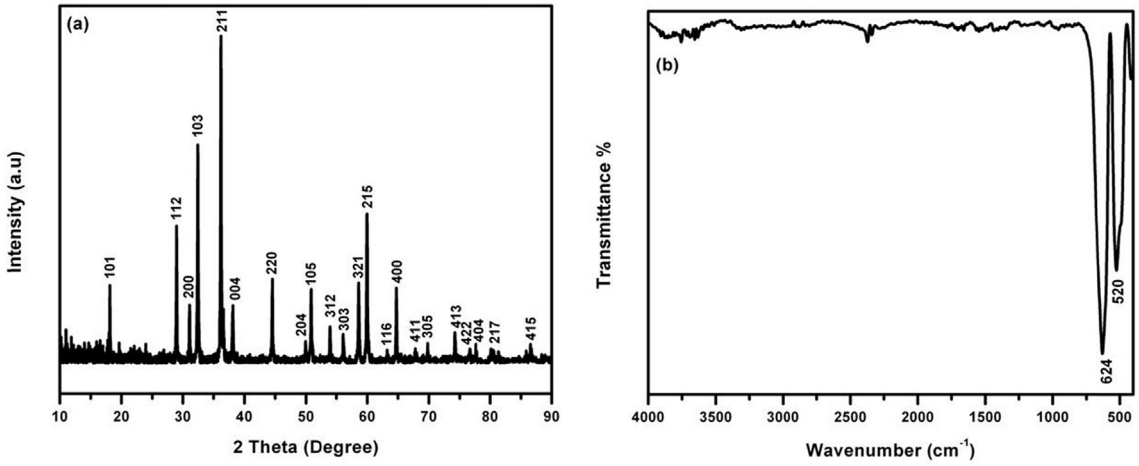

Fig. 2. (a) X-Ray diffraction pattern and (b) Fourier transform infrared spectrum of as prepared Mn_3O_4.

the exposure period of 1 h to ensure their steady state potential and then potentiodynamic polarization was carried out. The potentiodynamic condition corresponds to ±200 mV from the OCP with scan rate of 1 mV s^{-1}.

Corrosion current density was obtained from Rp and the slope of polarization curve was obtained by using the following relationship equation (1) [29].

$$i_{corr} = \frac{\beta a \cdot \beta c}{2.303\, Rp\, (\beta a + \beta c)} = \frac{B}{Rp} \quad (1)$$

where βa and βc is the anodic and cathodic slope of the polarization curve.

Electrochemical impedance spectra were measured in the frequency range of 0.1 Hz–100 kHz with AC amplitude of 5 mV and 30 reading per decade with respect to SCE and FPE using three electrodes cell setup was described above. The polarization resistance (Rp in Ω.cm^2) was measured at the lower frequency region using curve fitting method by using ACM software.

2.7. Steel corrosion monitoring in cement mortar specimen

In order to assess the real time use of FPE for corrosion assessment of steel rebar in concrete, we used concrete mortar specimen which was similar to our previous studies [30]. In brief it was discussed as follows. Ordinary portland cement (OPC); composition is given in Table 1. Thermo mechanically treated (TMT) rebar's (50 mm length and 12 mm dia) and locally available river sands were used. Cement mortar of 10 × 10 × 10 cm was prepared by using of concrete mix consists of 1:2.75:0.5 of cement, sand and water. For inducing of corrosion NaCl was mixed 0, 1, 2 and 3% with water. Before embedding the steel rebar was cleaned by picking solution consisting of hydrochloric acid, antimony trioxide and stannous chloride which was described in ASTM G1 and electrical lead was taken from one end. In order to avoid exposing of electrical contact in cement mortar, this was sealed using epoxy resin. Schematic illustration of as prepared concrete cube shown in Fig. 1a and it was is similar to Fig. 2a of our previous studies [30]. The specimens were demoulded after 24 h and then cured in distilled water at room temperature for 1 month.

Polarization and electrochemical impedance measurements were carried out using three electrode cell setup, in which, steel rebar embedded in concrete cube serve as working electrode, stainless steel covered around the concrete cube serve as counter electrode and FPE serve as embedded (in-situ) reference electrode. 0.04 N NaOH solution was used as electrolyte. Fig. 1a of bottom one and Fig. 1b shows the schematic and experimental setup of electrochemical measurements which is similar to our previous studies

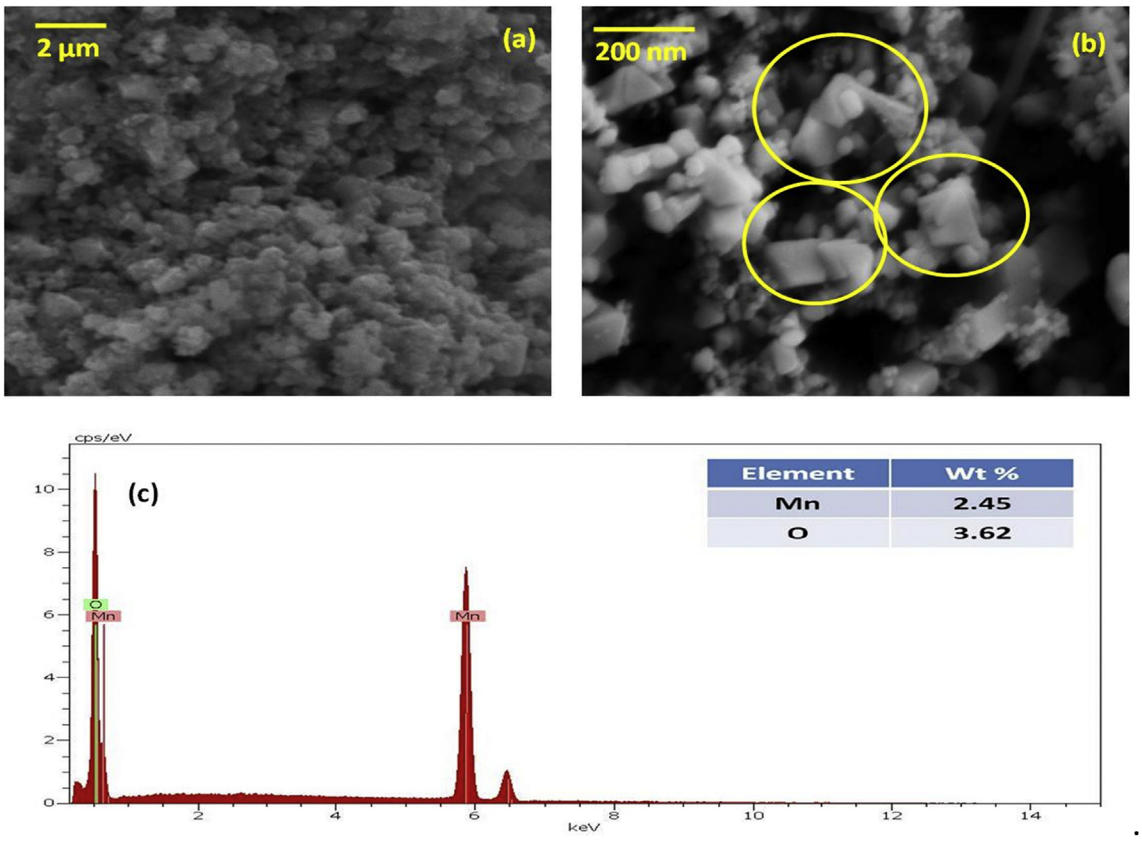

Fig. 3. (a) SEM (b) FESEM images and (c) Energy dispersive X-ray spectrum of as prepared Mn_3O_4.

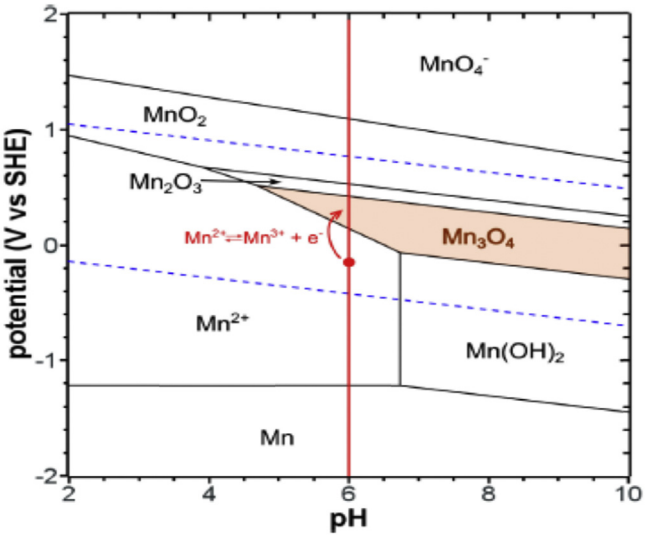

Fig. 4. E-pH (Pourbaix) diagram of 0.2 M Mn–H_2O system at 80 °C. The red vertical line represents the chemistry of the electrolyte used in this study. Reprinted with permission from Ref. [35]. Copyright (2014) American Chemical Society.

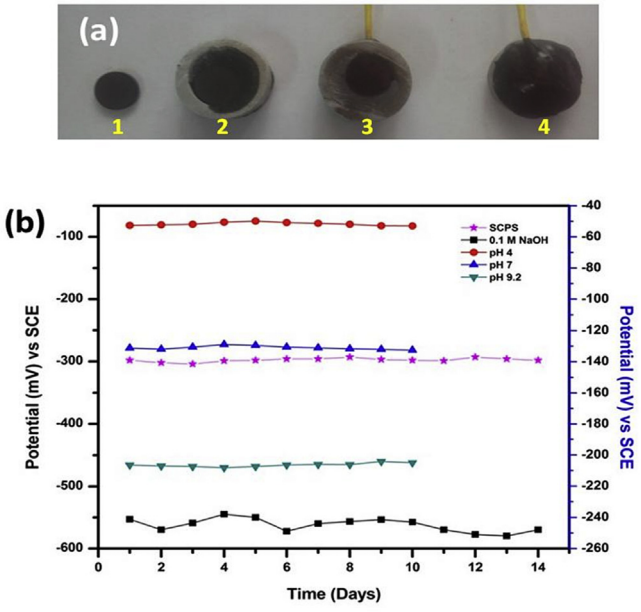

Fig. 5. (a) Photographs of PVC-epoxy molded fabricated Mn_3O_4 pellet electrode (1-Mn_3O_4 pellet, 2- Mn_3O_4 pellet embedded in PVC substrate, 3- front view of fabricated electrode and 4-back view of fabricated electrode) and (b) measured potential of FPE in 0.1 M NaOH and various pH solutions with respect SCE.

[30]. A potentiodynamic polarization condition corresponds to ± 200 mV from the OCP with scan rate of 1 mV s^{-1}. Electrochemical impedance spectra were measured in the frequency range of 0.1 Hz–100 kHz with AC amplitude of 5 mV and 30 reading per decade. In order to compare the results of FPE, similar experiments were also conducted using conventional SCE as ex-situ reference electrode.

3. Results and discussion

3.1. Structure and morphology of Mn_3O_4

Fig. 2a shows the X-ray diffractions pattern of as prepared Mn_3O_4 powder. In which, the diffraction patterns (101), (112), (200), (103), (211), (004), (220), (204), (105), (312), (303), (321), (215), (116), (400), (411), (305), (413), (422), (404), (217) and (415) diffraction planes are observed. These highly intensive narrow peaks coincide with the tetragonal Mn_3O_4 (JCPDS file No 24-0734). No other peaks of MnO_x impurities phase are detected. The well-defined sharp peaks suggest as prepared Mn_3O_4 well crystalline and good purity.

In order to get more information about prepared Mn_3O_4, Fourier transform infrared spectra (FTIR) studies were performed and shown in Fig. 2b. In which, the two major peaks are observed in the region of 400–700 cm^{-1}. The peaks around at 624 cm^{-1} and 520 cm^{-1} in which corresponds to the coupling of Mn–O stretching of tetrahedral and octahedral sites, respectively. These results is closely resemble to the recent literature of F. A. Al Sagheer et al. and K. Subramani et al. [31,32]. These results support X-ray diffraction studies and suggest the formation of Mn_3O_4 phase at lower temperature [31].

Fig. 3 shows the SEM and FESEM images of Mn_3O_4 sample. At low magnification (Fig. 3a) as prepared sample exhibits sponge like morphology [33]. At high magnification (Fig. 3b), it can be seen that the sponge likes structures are consists of agglomerated Mn_3O_4 tetragonal bipyramids [34]. In order to investigate the composition of Mn_3O_4, we performed Energy dispersive X-ray spectroscopic analysis (EDAX) and it can be shown in Fig. 3. It conform that samples purely consist of Mn and O with wt% ratio of 2.45:3.62; which is close to the empirical ratio of 3:4 chemical constituents.

3.2. The prospective use of Mn_3O_4 in alkaline environment

Pourbaix diagram is a well-known tool to assess the possible stable phase at equilibrium in aqueous electrochemical system. In this regards the potential vs. pH diagram of Mn–H_2O system is shown in Fig. 4 which shows the possible thermodynamic stability, redox couples, phase and ionic species at different pH values. Accordingly, the Mn_3O_4 was chosen in this study, due to their thermodynamic stability of Mn in Mn_3O_4 state at high pH regions. Mn_3O_4 reverse disproportionation and $Mn(OH)_2$ should not occurs at solution [35,36]. It gives possible stability status at high alkaline concrete like environment. In addition, the different phase of Mn in aqueous medium, Mn_3O_4 phase exhibits more stability in wide range of pH and above the ordinary room temperature. Further, the cyclic voltammogram of Mn_3O_4in aqueous neutral and high alkaline medium pH medium shows evidence of non-redox reaction behavior at the applied potentials widow of 0–1 V with respect to RHE (Reversible Hydrogen Electrode, it has potential 0 V in all pH range [37]) [16,38,39]. In this, characteristics are most suitable and offer new usage in high alkaline concrete like environment. Because of the concrete environment pH is found in the range of ~12.5–13.5.

3.2.1. Potential performance of fabricated Mn_3O_4 solid electrode

In general, the reference electrode potential were described by Nernst equation which is shown in equation (2) [40–42].

$$E_{M^{n+}/M} = E^{\circ} + \frac{RT}{nF} \ln \frac{a_{M^{n+}}}{a_M} \quad (2)$$

Where M^{n+} and M are the activities of the oxidized and reduced species respectively. E, R, T, n and F stands for the electrode potential, gas constant, temperature, number of electron transfer during the oxidation and reduction, Faraday's constant respectively. Let us consider the conventional reference electrodes of Hg/Ha_2Cl_2, Ag/AgCl and Hg/HgO and its electrolytes of KCl, NaCl, NaOH and KOH [43]. In these conventional reference electrode, the potential arises due to the reversible redox reaction active species and the activities of electrolyte ions like Cl^- and OH^- and hence, it follows the Nernst equation to represent the equilibrium potential and vice versa [22,43].

However, the Nernst's law applies quite well for neutral and acidic solutions ($1 < pH < 7$). Nevertheless in alkaline solutions this linear relationship with pH is no more valid (especially in concrete medium which have a pH of ~12.5–13.5) [19]. So, the Nernst laws cannot be used in this case to determine the half-cell reaction of the reference electrode when it is to be made up of special noble metals like Pt, Ag and carbon and addition to this when it is to be used in special environment like solid or gas [44,45]. The activities of oxidized and reduced species are unknown and hence the behavior of the electrode is unpredictable by the Nernst law but it exhibits stable potential behavior with time [14,17,42]. This kind of reference electrodes are said to be pseudo reference electrode. Hence, most of the solid state reference electrodes are similar to pseudo reference electrode and it gives potential with respect to pH of test medium [14,46]. This present study describes the possible utilization of Mn_3O_4 materials to fabricate the solid state reference electrode for corrosion monitoring of steel rebar in concrete structure. It has the solid component of Mn_3O_4 alone in the form of pellet. Hence, it is able to give some potential like pseudo reference electrode without any redox reaction like MMO reference electrode studied by G. S. Duffo et al., and U. Guth et al. [14,17,46]. And thereby the Mn_3O_4 is believed to be thermodynamically highly stable in alkaline pH it was described by the Pourbaix diagram [35,36].

In most of the embeddable reference electrode potential depends on the concrete environment and which may not stable for long-term due to the high pH and chlorides [47]. So, before embedding into the concrete, evaluation of potential stability in concrete like high alkaline environment was important factor. In order to investigate the potential stability of FPE in high alkaline environment (similar to concrete) for corrosion monitoring, we took alkaline solutions such as 0.1 M NaOH and synthetic concrete pore solution (0.3 M KOH, 0.1 M NaOH and 0.01 M $Ca(OH)_2$; pH ~13). Fig. 5b shows the measured potential of FPE with respect to SCE. It can be seen that, the FPE potential was found to be −250 mV and −300 mV with respect to SCE in 0.1 M NaOH and synthetic concrete pore solution respectively. At the same time the measured potential was found stable without much deviation. It indicates that the fabricated solid state reference electrode furnish stable potential at the equilibrium state in high alkaline aqueous medium and this results closest to thermodynamic stable state of Mn in the form of Mn_3O_4 phase [35,36].

Addition to the alkaline solution studies, the potential behavior of FPE were studied in different pH solution which includes of pH of 4, 7 and 9.2. Fig. 5b shows the FPE potential (vs. SCE) in different pH solution for the immersion periods of 10 days. In these studies, the potential of FPE was found pH dependent, in which the lower pH at 4 around −50 mV was found. The increase of pH from acid to alkaline measured potential value was increased in negative direction and it was found to be −130 mV and −204 mV at pH 7 and 9.2 respectively. No large significant potential changes were

Table 1
Chemical composition of as used ordinary portland cement (OPC).

Constituents	CaO	SiO_2	Al_2O_3	Fe_2O_3	MgO	SO_3	LOI
%	62.70	20.80	5.40	4.60	0.60	2.60	3.30

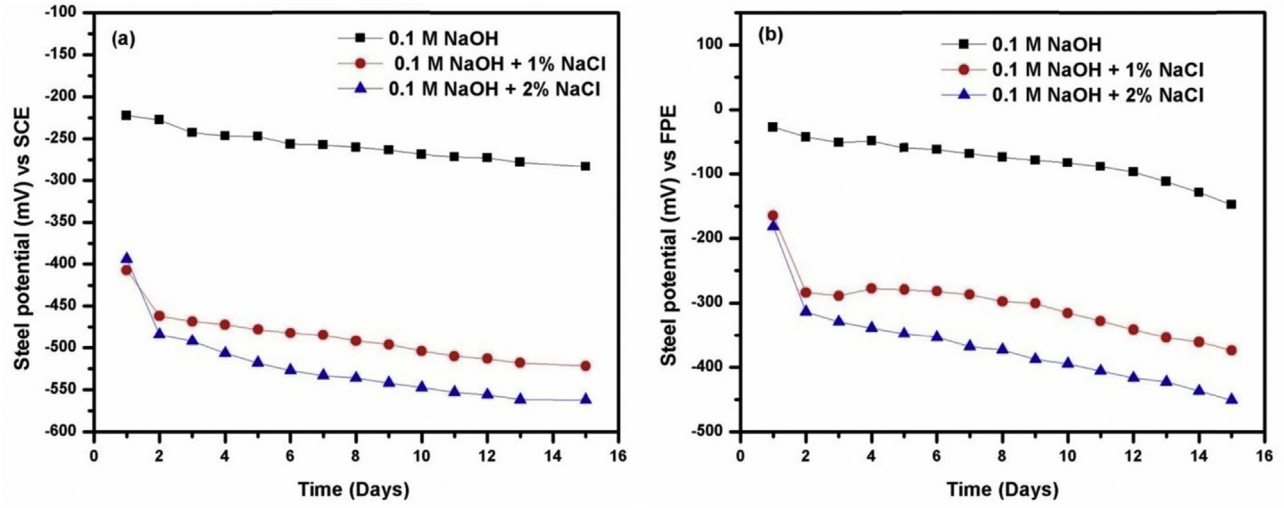

Fig. 6. Measured steel potential in different solution with respect to (a) SCE and (b) FPE.

observed during the exposure periods in different pH solutions. These results in were accordance with earlier studies of potential of MMO electrode for corrosion monitoring in reinforced concrete structures [14,17,48]. The influence of other metal cations and anions solution toward the influence of potential was not studied in this study and it was beyond the scope of study. This potential performance evolution of test solution of alkaline solution and SCP solution were taken from the literature studied by G. S. Duffo et al., Guofu Qiao et al., H. Yi et al., H. Yu et al., Shi-Gang Dong et al. and S. Muralidharan et al. [12–15,17,42,48].

Accordingly these studies results suggest that the FPE deliver stable potential in high alkaline medium and their potential linearly vary with respect to pH of test solution. These are very suitable high alkaline medium concrete medium.

3.2.2. *Corrosion potential sensing in active and passive condition of steel*

In order to evaluate the corrosion monitoring of steel rebar in concrete like high alkaline environment, we exposed steel rebar in 0.1 M NaOH with 1% and 2% NaCl (active) and without NaCl (passive). The steel rebar potential was measured with respect SCE and FPE, that's similar to ASTM C876. From the measured potentials (Fig. 6) the status steel rebar was assessed and described as follows. In which Fig. 6a the measured potential of steel with respect to SCE, increase of potential in negative direction from −220 mV to −250 mV in 0.1 M NaOH and −400 mV to −500 mV indicates, the

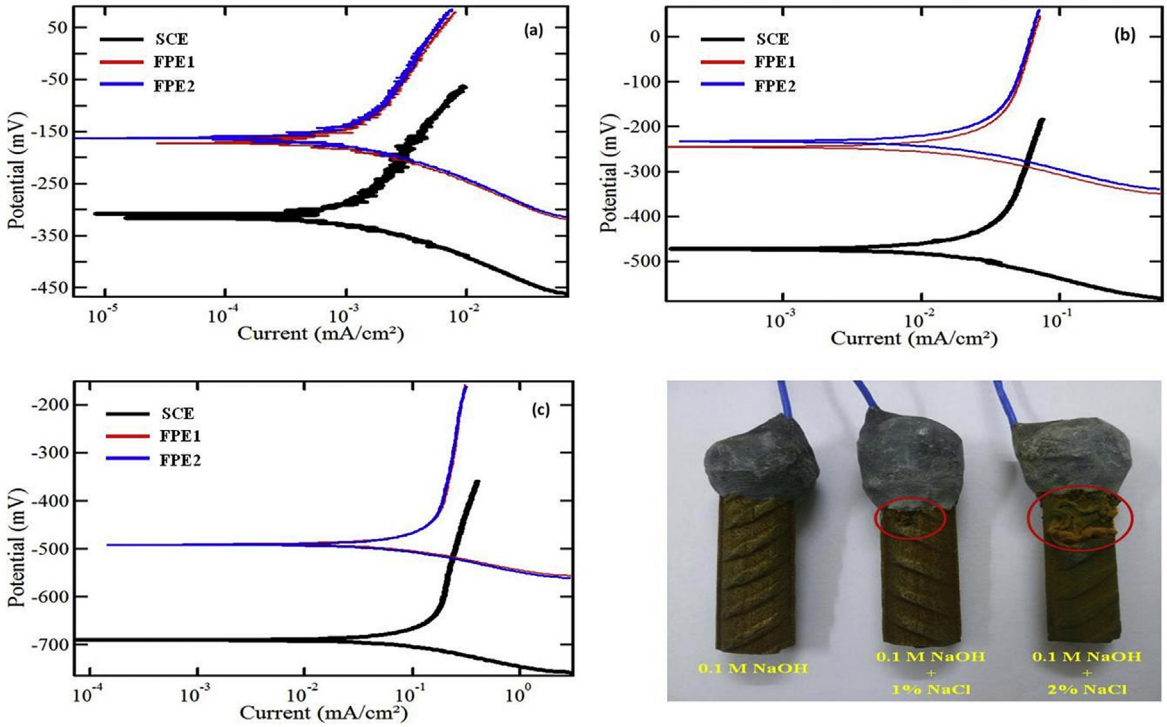

Fig. 7. Measured steel potential with respect to SCE and FPE in 0.1 M NaOH and 1% NaCl and 2% NaCl solution.

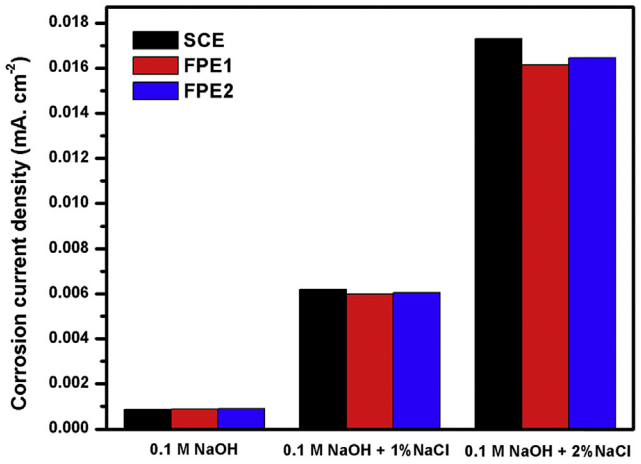

Fig. 8. Steel rebar corrosion current density measured with respect SCE and FPE in 0.1 M NaOH and 1% NaCl and 2% NaCl solution.

Table 2
Polarization parameters of steel with respect to SCE and FPE in various solutions.

Solution	Reference electrode	E_{corr} (mV)	i_{corr} (mA cm^{-2})	β_a (mV dec^{-1})	β_c (mV dec^{-1})
0.1 M NaOH	SCE	−309	0.000869	270	41
	FPE1	−172	0.000889	319	52
	FPE2	−162	0.000900	331	36
0.1 M NaOH + 1% NaCl	SCE	−473	0.006184	786	29
	FPE1	−234	0.000889	1016	42
	FPE2	−246	0.006043	820	28
0.1 M NaOH + 2% NaCl	SCE	−690	0.017304	7125	25
	FPE1	−459	0.016138	1026	20
	FPE2	−489	0.016451	1387	24

FPE1 and 2: Fabricated Pellet Electrode 1 and 2.

steel rebar moving towards active state from the passive state. Behalf of these results of half-cell potential the visual observation of corrosion status can be shown Fig. 7d by photographic image. From this study, the high alkaline immersion of steel itself has passive nature to corrosion compared to the presence of Cl^- content and the long term exposure increases the corrosion of steel rebar. In addition, the increase of steel potential vs. SCE in negative direction is directly proportional to the corrosion status [8].

Fig. 6b shows the steel rebar potential measured with respect to FPE. In which the passive state of state steel rebar potential was found to be in the range of −25 to −120 mV. In the case of active chloride environment, the steel rebar potential was increased in negative direction from the initial potential of −160 mV to −300 mV. This increasing of potential in negative direction indicates that the rebar corrosion rate increases with respect to exposing days in presence of Cl^-. These results are coinciding with the corrosion current density measured with respect SCE and FPE by potentiodynamic polarization studies it can be shown in Fig. 8.

These results are very similar to corrosion potential measurement with respect to SCE, the FPE having the ability to differentiate the steel rebar in corroding environment, whether it is in an active or passive state.

3.2.3. Corrosion studies by potentiodynamic polarization method in solution

To investigate the fabricated electrode suitability for corrosion monitoring of steel in high alkaline environment, we performed a potentiodynamic polarization studies and the result were compared with conventional SCE in various solutions after exposure of 15 days. Fig. 7 shows the obtained Tafel curves of E_{corr} (vs SCE and FPE) vs log i_{corr} and the resulting parameters are given in Table 2. In the case of steel exposed in 0.1 M NaOH (Fig. 7a) the corrosion potential (E_{corr}) and current density (i_{corr}) was found to be −309 mV and 0.000869 mA cm^{-2} with respect to SCE and −165 mV and 0.000900 mA cm^{-2} with respect to FPE. In another case of steel exposed in 1% NaCl added solution E_{corr} and i_{corr} was found to be −470 mV and 0.006184 mA cm^{-2} with respect to SCE and −240 mV and 0.006000 mA cm^{-2} with FPE respectively. The lower corrosion potential (E_{corr}) and higher current density of (i_{corr}) indicates the active state of steel rebar in 1% NaCl with 0.1 M NaOH solution. When the chloride content in which of NaCl increased from 1% to 2% the corrosion rate are increased. This will increase the corrosion potential and corrosion current density. Fig. 8 shows the overall corrosion current density (i_{corr}) measured in different test solution with respect to SCE and FPE. It can be seen

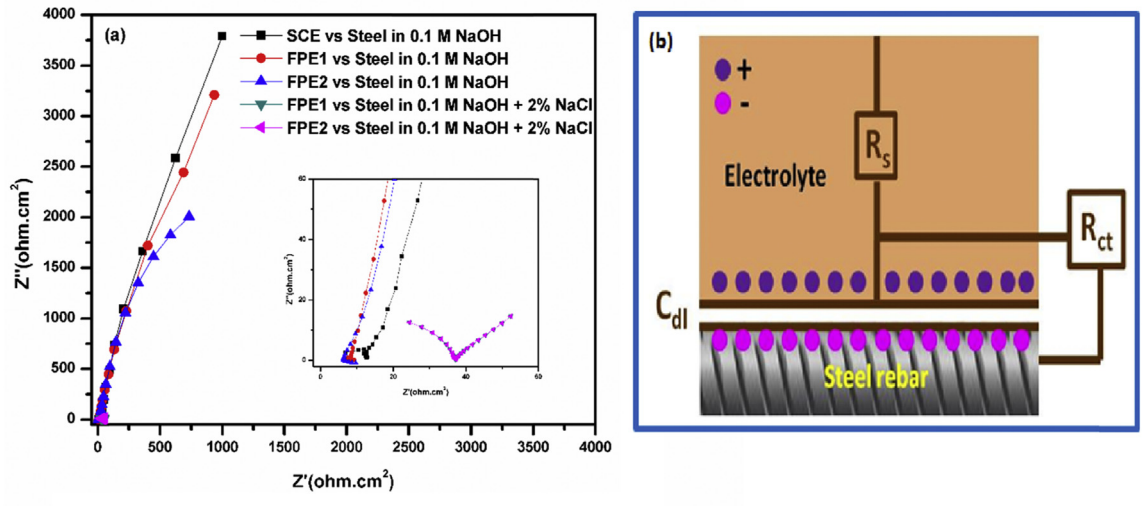

Fig. 9. (a) Electrochemical impedance plot of steel with respect to SCE and FPE in with 2% NaCl and without NaCl in 0.1 M NaOH and (b) Electrical equivalent circuit of model for the EIS of steel rebar in high alkaline medium.

Table 3
Electrochemical impedance parameters of steel rebar with respect to SCE and FPE.

Solution	Reference electrode	R_s (Ω cm^2)	R_{ct} (Ω cm^2)	C_{dl} (F cm^{-2})
0.1 M NaOH	SCE	9.1	5.8×10^3	4.9×10^{-4}
	FPE1	8.4	5.6×10^3	3.7×10^{-4}
	FPE2	4.9	5.6×10^3	4.8×10^{-4}
0.1 M NaOH + 2% NaCl	SCE	3.8	4.2×10^2	9.7×10^{-4}
	FPE1	2.5	4.4×10^3	6.9×10^{-4}
	FPE2	2.7	4.3×10^3	6.9×10^{-4}

FPE1 and 2: Fabricated Pellet Electrode 1 and 2.

that, the measured current density is repeatable and reproducible and is similar to the conventional SCE reference electrode. In this regards, the FPE electrode demonstrates the ability to differentiate active and passive state steel rebar's in concrete like high alkaline environment.

3.2.4. Impedance measurements

Corrosion status of steel rebar was further studied by electrochemical impedance spectroscopic (EIS) method and Fig. 9a shows the results of Nyquist plots measured in 0.1 M NaOH with 2% NaCl and without NaCl measured with respect to SCE and FPE. The resulting parameters are shown in Table 3. It can be seen that, the measured corrosion behavior of steel in both fabricated electrode showed same values and the results closely resembled to SCE.

We suggest the schematic equivalent circuit of Fig. 9b to interpret electrochemical impedance behavior and its derived parameters of steel rebar which is similar to recent studies [49,50], whereas R_s, R_{ct} and C_{dl} are the solution resistance, charge transferee resistance and double layer capacitance of system respectively. For in this case, basis of results the lower value of R_s in the presence of 2% NaCl than compared to 0.1 M NaOH indicate the active corrosion state of steel rebar [49] and the steel rebar sensitive to electrolyte and breakdown the steel rebar passive film that means defective surface of steel rebar. These EIS results support the relative use of FPE in corrosion status assessment studies similar to SCE and it suggest that, strong correlation exists between the SCE and FPE.

3.3. Corrosion studies by potentiodynamic polarization method in concrete cube

The effectiveness of FPE as embeddable in-situ corrosion status assessment of steel rebar in concrete structure were studied with rebar in the concrete cube (Fig. 1a) by the FPE as in-situ reference electrode and the results were compared with the SCE as ex-situ reference electrode through the potentiodynamic polarization method. Table 4 summaries the results of steel rebar corrosion potential (E_{corr}) concrete cube exposed in distilled water (passive) and 3% NaCl in water. The increase of corrosion potential in the negative direction with respect to SCE and FPE clearly states that the steel rebar undergoes corrosion with increasing exposing time and it is also found that the ability of FPE to differentiate the active and passive state of steel rebar is similar to the SCE.

Table 4
Measured corrosion potential of steel in concrete mortar.

Measured at the day of	Specimen	Corrosion potential (E_{corr}) mV	
		SCE	FPE
33rd	Bare (Passive)	−247	−235
	3% NaCl added (Active)	−436	−308
67th	Bare (Passive)	−310	−302
	3% NaCl added (Active)	−483	−372

4. Conclusion

In this present study, Mn_3O_4 based pellet reference electrode was successfully fabricated and characterized in high alkaline solution environment. The electrochemical studies reveal that FPE gives pH dependable potential. Corrosion monitoring studies of steel rebar was conducted through the potentiodynamic polarization and electrochemical impedance method and the results were compared with conventional SCE reference electrode. The resulting data showed the better characteristics of FPE in high alkaline concrete like environment. When it is used in steel rebar corrosion assessment of concrete structures, it can easily differentiate the passive and active state of steel rebar.

Acknowledgement

We thank Council of Scientific Industrial Research (CSIR), India, for the financial support through MULTIFUN (CSC-0101) Project.

References

[1] S. Grousset, F. Kergourlay, D. Neff, E. Foy, J.L. Gallias, S. Reguer, P. Dillmann, A. Noumowe, In situ monitoring of corrosion processes by coupled micro-XRF/micro-XRD mapping to understand the degradation mechanisms of reinforcing bars in hydraulic binders from historic monuments, J. Anal. At. Spectrom. 30 (2015) 721–729.
[2] G.D. Rong, G.H. Rong, S.H. Ruo, J.L. Chang, Situ measurement of Cl^- concentrations and pH at the reinforcing steel/concrete interface by combination sensors, Anal. Chem. 78 (2006) 3179–3185.
[3] O.R. Batic, J.D. Sota, J.L. Fernandez, A.B. Del, R. Romagnoli, Rebar corrosion in mortars containing calcareous filler, Ind. Eng. Chem. Res. 49 (2010) 8488–8494.
[4] Ji-Hong Yooa, Zin-Taek Parka, Jung-Gu Kima, Lan Chung, Development of a galvanic sensor system for detecting the corrosion damage of the steel embedded in concrete structures: part 1. Laboratory tests to correlate galvanic current with actual damage, Cem. Concr. Res. 33 (2003) 2057–2062.
[5] Zin-Taek Park, Yoon-Seok Choi, Jung-Gu Kim, Lan Chung, Development of a galvanic sensor system for detecting the corrosion damage of the steel embedded in concrete structure part 2. Laboratory electrochemical testing of sensors in concrete, Cem. Concr. Res. 35 (2005) 1814–1819.
[6] W.S. Ha, V. Saraswathy, Corrosion monitoring of reinforced concrete structures – a review, Int. J. Electrochem. Sci. 2 (2007) 1–28.
[7] K.V. Sanjeev, S.B. Sudhir, A. Saleem, Hindawi Publishing Corporation, Monitoring corrosion of steel bars in reinforced concrete structures, Sci. World J. (2014), http://dx.doi.org/10.1155/2014/957904. Article ID 957904.
[8] M.W. John, V. Øystein, Sensor systems for use in reinforced concrete structures, Constr. Build. Mater. 18 (2004) 351–358.
[9] S.P. Karthick, S. Muralidharan, V.Saraswathy, K. Thangavel, Long-term relative performance of embedded sensor and surface mounted electrode for corrosion monitoring of steel in concrete structures, Sens. Actuators B 192 (2014) 303–309.
[10] S. Muralidharan, V. Saraswathy, L. John Berchmans, K. Thangavel, Y.A. Ki, Nickel ferrite ($NiFe_2O_4$): a possible candidate material as reference electrode for corrosion monitoring of steel in concrete environments, Sens. Actuators B 145 (2010) 225–231.
[11] Q. Guofu, H. Yi, S. Guangping, L. Hui, O. Jinping, Electrochemical characterization of the solid-state reference electrode based on $NiFe_2O_4$ film for the corrosion monitoring of RC structures, Sens. Actuators B 168 (2012) 172–177.
[12] H. Yi, S. Guangping, Preparation of the $NiFe_2O_4$ electrochemical film for the solid-state reference electrode based on EB-PVD, Appl. Surf. Sci. 258 (2012) 8934–8939.
[13] H. Yu, L. Caseres, An embedded multi-parameter corrosion sensor for reinforced concrete structures, Mater. Corros. 63 (11) (2012) 1011–1016.

[14] G.S. Duffo, S.B. Farina, C.M. Giordano, Embeddable reference electrodes for corrosion monitoring of reinforced concrete structures, Mater. Corros. 61 (6) (2010) 480–489.
[15] G.D. Shi, J.L. Chang, G.H. Rong, Q.L. Lan, G.D. Rong, Effective monitoring of corrosion in reinforcing steel in concrete constructions by a multifunctional sensor, Electrochim. Acta 56 (2011) 1881–1888.
[16] B. Sharmistha, D.J. Thomson, G.E. Bridges, A wireless embedded passive sensor for monitoring the corrosion potential of reinforcing steel, Smart Mater. Struct. 22 (2013) 075019.
[17] U. Guth, F. Gerlach, M. Decker, W. Oelßner, W. Vonau, Solid-state reference electrodes for potentiometric sensors, J. Solid. State Electrochem. 13 (2009) 27–39.
[18] Anna Kisiel, Honorata Marcisz, Agata Michalska, Krzysztof Maksymiuk, All-solid-state reference electrodes based on conducting polymers, Analyst 130 (2005) 1655–1662.
[19] Stéphanie Lorant, Claude Bohnke, Michaël Roffat, Odile Bohnke, New concept of an all-solid-state reference electrode using a film of lithium lanthanum titanium oxide (LLTO), Electrochim. Acta 80 (2012) 418–425.
[20] Jui-Fu Cheng, Jung-Chuan Chou, Tai-Ping Sun, Shen-Kan Hsiung, All-solid-state separated potassium electrode based on SnO_2/ITO glass, J. Electrochem. Soc. 154 (11) (2007) J369–J374.
[21] V. Maruthapandian, S. Muralidharan, V. Saraswathy, Liquid-free alkaline gel filled reference electrode based on Cr_2O_3 spheres, Indian J. Chem. 54A (2015) 1215–1220.
[22] György Inzelt, Andrzej Lewenstam, Fritz Scholz, Handbook of Reference Electrodes, Springer, Heidelberg New York Dordrecht London, 2013, p. 331.
[23] Q. Li, G. Luo, Y. Shu, Response of nanosized cobalt oxide electrodes as pH sensors, Anal. Chim. Acta 409 (2000) 137–142.
[24] G.K. Kenneth, J.T. Michael, P.C. James, Sputtered thin-film pH electrodes of platinum, palladium, ruthenium, and iridium oxides, Sens. Actuators B 28 (1995) 167–172.
[25] D. Jingjing, Z. Yao, C. Sheng, T. Youhong, J. Mietek, Q. Shizhang, Mesoporous hybrid material composed of Mn_3O_4 nanoparticles on nitrogen-doped graphene for highly efficient oxygen reduction reaction, Chem. Commun. 49 (2013) 7705–7707.
[26] J. Guoqiang, X. Yunhua, C.L. Li, W. Chunsheng, R.Z. Michael, Mn_3O_4 hollow spheres for lithium-ion batteries with high rate and capacity, J. Mater. Chem. A 2 (2014) 4627–4632.
[27] G. Yelena, J.C. Chia, N. Dennis, M.C. Bruce, F.J. Thomas, Mn_3O_4 supported on glassy carbon: an active non-precious metal catalyst for the oxygen reduction reaction, ACS Catal. 2 (2012) 2687–2694.
[28] Balasubramaniam Gnana Sundara Raj, Abdullah M. Asiri, Jerry J. Wuc, Sambandam Anandan, Synthesis of Mn_3O_4 nanoparticles via chemical precipitation approach for supercapacitor application, J. Alloys Compd. 636 (2015) 234–240.
[29] V. Barranco, J.S. Feliu, S. Feliu, EIS study of the corrosion behaviour of zinc-based coatings on steel in quiescent 3% NaCl solution. Part 1: directly exposed coatings, Corros. Sci. 46 (2004) 2203–2220.
[30] V. Maruthapandian, S. Muralidharan, V. Saraswathy, Spinel $NiFe_2O_4$ based solid state embeddable reference electrode for corrosion monitoring of reinforced concrete structures, Constr. Build. Mater. 107 (2016) 28–37.
[31] F.A. Al Sagheer, M.A. Hasan, L. Pasupulety, M.I. Zaki, Low-temperature synthesis of hausmannite Mn_3O_4, J. Mater. Sci. Lett. 18 (1999) 209–211.
[32] K. Subramani, D. Jeyakumar, M. Sathish, Manganese hexacyanoferrate derived Mn_3O_4 nanocubes–reduced graphene oxide nanocomposites and their charge storage characteristics in supercapacitors, Phys. Chem. Chem. Phys. 16 (2014) 4952–4961.
[33] G. Jie, A.L. Michael, D.A. Hector, Spongelike nanosized Mn_3O_4 as a high-capacity anode material for rechargeable lithium batteries, Chem. Mater. 23 (2011) 3223–3227.
[34] L. Taotao, G. Chunli, S. Bo, L. Ting, L. Yonggang, H. Lifeng, W. Yinghui, Well-shaped Mn_3O_4 tetragonal bipyramids with good performance for lithium ion batteries, J. Mater. Chem. A 3 (2015) 7248–7254.
[35] A.K. Jakub, P.S. Ian, M.W. Matthew, A.S. Jay, Electrochemical synthesis and nonvolatile resistance switching of Mn_3O_4 thin films, Chem. Mater. 26 (2014) 4425–4432.
[36] C.M. Robert, B.G. James, Assembly of a robust and economical MnO_2-based reference electrode, J. Chem. Educ. 92 (1) (2015) 110–115.
[37] A.P. Andrew, A.P. Frank, S. Felix, R. Jan, K.N. Jens, How copper catalyzes the electroreduction of carbon dioxide into hydrocarbon fuels, Energy Environ. Sci. 3 (2010) 1311–1315.
[38] D.P. Dubal, D.S. Dhawale, R.R. Salunkhe, S.M. Pawar, C.D. Lokhande, A novel chemical synthesis and characterization of Mn_3O_4 thin films for super-capacitor application, Appl. Surf. Sci. 256 (2010) 4411–4416.
[39] R. Alejandra, H. Philipp, S. Diana, M.M. Matthias, B. Peter, F. Sebastian, Evaluation of MnO_x, Mn_2O_3, and Mn_3O_4 electrodeposited films for the oxygen evolution reaction of water, J. Phys. Chem. C 118 (2014) 14073–14081.
[40] F.J. Vidal-Iglesias, Jose Solla-Gullon, A. Rodes, E. Herrero, A. Aldaz, Understanding the Nernst equation and other electrochemical concepts: an easy experimental approach for students, J. Chem. Educ. 89 (2012) 936–939.
[41] M. Waleed Shinwari, David Zhitomirsky, Imran A. Deen, P.R. Selvaganapathy, M. Jamal Deen, D. Landheer, Microfabricated reference electrodes and their biosensing applications, Sensors (Basel) 10 (3) (2010) 1679–1715.
[42] G. Qiao, H. Xiao, Y. Hong, Y. Qiu, Preparation and characterization of the solid-state Ag/AgCl reference electrode for RC structures, Sens. Rev. 32 (2) (2012) 118–122.
[43] R.A. Scott, Applications of Physical Methods to Inorganic and Bioinorganic Chemistry, John Wiley and Sons, 2007, p. 23.
[44] K.K. Kasem, S. Jones, Platinum as a reference electrode in electrochemical measurements, Platin. Met. Rev. 52 (2) (2008) 100–106.
[45] A.A.G.F. Beati, R.M. Reis, R.S. Rocha, M.R.V. Lanza, Development and evaluation of a pseudoreference Pt//Ag/AgCl, electrode for electrochemical systems, Ind. Eng. Chem. Res. 51 (2012) 5367–5371.
[46] G.S. Duffó, S.B. Farina, C.M. Giordano, Characterization of solid embeddable reference electrodes for corrosion monitoring in reinforced concrete structures, Electrochim. Acta 54 (2009) 1010–1020.
[47] G.S. Duffó, S.B. Farina, Development of an embeddable sensor to monitor the corrosion process of new and existing reinforced concrete structures, Constr. Build. Mater. 23 (2009) 2746–2751.
[48] S. Muralidharan, H.H. Tae, H.B. Jeong, C.H. Yoon, G.L. Hyun, W.P. Kyung, K.K. Dae, Electrochemical studies on the performance characteristics of solid metal–metal oxide reference sensor for concrete environments, Sens. Actuators B 113 (2006) 187–193.
[49] R. Leiva-Garcia, J.C.S. Fernandes, M.J. Muñoz-Portero, J. García-Anton, Study of the sensitisation process of a duplex stainless steel (UNS 1.4462) by means of confocal microscopy and localised electrochemical techniques, Corros. Sci. 94 (2015) 327–341.
[50] H. Esam, N.N. Tharangattu, T.T. Jose Jaime, V. Soumya, V. Robert, M.A. Pulickel, Marine corrosion protective coatings of hexagonal boron nitride thin films on stainless steel, ACS Appl. Mater. Interfaces 5 (2013) 4129–4135.